Korean J. Chem. Eng., 32(8), 1606-1612 (2015)
DOI: 10.1007/s11814-014-0373-z

pISSN: 0256-1115
eISSN: 1975-7220

Adsorptive removal of acetaminophen and diclofenac using NaX nanozeolites synthesized by microwave method

Leila Roshanfekr Rad*, Mohammad Irani,†, and Roya Barzegar****

*Department of Chemistry, Guilan Science and Research Branch, Islamic Azad University, Guilan, Iran
**Department of Chemical Engineering, Amirkabir University of Technology (Tehran Polytechnic), Tehran, Iran
(*Received 12 September 2014 • accepted 9 December 2014*)

Abstract−The adsorption of acetaminophen (ATP) and diclofenac (DCF) from aqueous systems was investigated using NaX nanozeolites synthesized by microwave heating method. The synthesized nanoparticles were characterized by powder X-ray diffraction (XRD), scanning electronic microscopy (SEM), Brunauer-Emmet-Teller (BET), X-ray fluorescence (XRF) and dynamic light scattering (DLS) analysis. The effect of sorption parameters including adsorbent dosage, contact time, initial concentration and temperature on the removal of ATP and DCF was studied in a batch system. The kinetic data were analyzed using pseudo-first-order, pseudo-second-order and double-exponential kinetic models. The Langmuir, Freundlich, Temkin and Dubinin-Radushkevich isotherm models were used to describe the equilibrium data of ATP and DCF. Thermodynamic parameters were determined to evaluate the nature of ATP and DCF sorption by NaX nanozeolites. The results showed that both ATP and DCF sorption processes were endothermic and spontaneous in the studied conditions. The reusability of NaX nanozeolites was also evaluated after four sorption-desorption cycles. Moreover, this study provides a promising adsorbent with higher efficiency for adsorption of pharmaceutical compounds.

Keywords: Acetaminophen, Diclofenac, Adsorption, NaX Nanozeolites, Microwave

INTRODUCTION

The pharmaceutical residues in the water are considered as emerging pollutants [1-3]. Acetaminophen [(N-acetyl-4-aminophenol), ATP] and diclofenac [(2-[(2, 6-dichlorophenyl) amino] phenylacetic acid, DCF] are commonly used as analgesic and anti-inflammatory agents for humans and animals [4-6]. Very low concentrations of ATP and DCF are commonly detected in the surface water includes rivers, drinking water, and groundwater [7,8]. The presence of trace pharmaceuticals in drinking water has a toxic effect on human and animal health. Various processes including advanced oxidation [9], membrane filtration [10], biological treatment [11], photocatalytic degradation [12] and adsorption [13] have been used for the removal of organic pollutants from aqueous solution. Although advanced oxidation processes have been extensively used for the treatment of pharmaceutical wastes [14-16], these techniques are associated with problems such as excessive time requirements, high costs and high energy consumption. In this way, the adsorption process, due to its simplicity, moderate operational conditions and economic feasibility, could be an effective method for treatment of pharmaceutical wastes [13,17]. In recent years, researchers used various types of adsorbents such as activated carbon [18], zeolites [19], and mesoporous silica [20] for the removal of pharmaceutical wastes [21]. Zeolites, due to the ion exchange properties and their hydrophilic affinities as well as higher surface area, are widely used for adsorption of pharmaceutical compounds from aqueous systems [19,22]. In previous studies, researchers used various types of zeolites such as HFAU and NaY for the treatment of phenolic compounds from aqueous solution [23]. However, there is no report about the application of NaX nanozeolites for the removal of ATP and DCF from water.

The ability of any adsorbent depends on the surface area, chemical nature and polarity. Recently, nanometer-sized zeolites due to their exclusive properties, such as large external surface area, more accessible active sites as well as shorter diffusion pathways, have been widely used in adsorption process compared with micrometer-sized zeolite crystals [15]. Among several methods of synthesis of nanozeolites, the microwave heating method, due to rapid annealing of microwave sintering, produces smaller nanoparticles. For this, NaX nanozeolites are synthesized by microwave heating method to improve the ability of NaX nanozeolites for adsorption of pharmaceutical compounds.

In the present study, the potential of NaX nanozeolites for the removal of ATP and DCF from aqueous solutions was investigated. The influence of various experimental parameters including adsorbent dosage, contact time, initial concentration and temperature on ATP and DCF sorption using NaX nanozeolite, were studied to obtain the optimum conditions for the maximum adsorption efficiency. The nature of the adsorption process with respect to its isotherm (Langmuir, Freundlich, Temkin, and Redlich-Peterson), kinetics (pseudo-first-order, pseudo-second-order and double exponential models) and thermodynamics [Gibbs free energy change (ΔG^o),

†To whom correspondence should be addressed.
E-mail: irani_mo@ut.ac.ir

enthalpy change (ΔH^o) and entropy change (ΔS^o)] were also evaluated.

EXPERIMENTAL

1. Materials

Fumed silica (7 nm) and $NaAlO_2$ were purchased from Sigma-Aldrich. NaOH was obtained from Merck. Acetaminophen ($C_8H_9NO_2$) and diclofenac ($C_{14}H_{11}Cl_2NO_2$) were provided from Jalinous pharmaceutical company of Iran. Commercial NaX zeolite (Zeochem) was used through the experiments (Switzerland).

2. Synthesis of Nano NaX Zeolite

The NaX nanozeolites were synthesized according to the method described previously [24]. For synthesis of NaX nanozeolites using microwave heating method, first, the aluminosilicate gel was prepared by mixing of aluminate and silicate solutions together in the molar ratios of 5.5 Na_2O : 1.0 Al_2O_3 : 4.0 SiO_2 : 190 H_2O. Then, microwave heating proceeded at 90 °C for 3 h. After that, the prepared powder was washed with distilled water until pH value reached below 8.0, and finally dried at room temperature for 24 h.

3. Characterization of the NaX Nanozeolites

The powder's X-ray diffraction (XRD) patterns were recorded at 25 °C on a Philips instrument (X'pert diffractometer using CuKα radiation) with a scanning speed of 0.03° (2θ) min^{-1} to confirm NaX zeolite structure. The morphological analysis of the NaX nanozeolite was characterized using scanning electron microscopy (SEM, TESCAN, VEGA 3SB) after gold coating. The average diameter of nanozeolites was obtained by an image analyzer (Image-Proplus, Media Cybernetics). The XRF (PV 9500 instrument) was used to evaluate the elemental compositions of nanoparticles and determine Si/Al ratio. A chromium X-ray source operating at 200 kV/20 A was used. The pore volume, pore diameter and specific surface area of nanoparticles were also measured for the zeolite nanoparticles with nitrogen adsorption and BET method on a Quantachrome Autosorb-1 instrument. Also, the hydrodynamic diameter and size distribution of the NaX zeolite nanoparticles were determined by dynamic light scattering (DLS) using a Malvern Zetasizer Nano (Malvern Instruments, Worcestershire) (Wavelength: 632.8 nm, Scattering Angle: 173°). The point of zero charge (pH_{pzc}) was determined according to Irani et al. [25] for determination of pH_{pzc}. The concentrations of pharmaceutical compounds were determined using a UV-Vis spectrophotometer (JAS.CO V-530, wavelengths 248 and 276 nm; ATP and DCF). Deionized water was used throughout this work.

4. Adsorption Experiments

The adsorption efficiency of ATP and DCF was studied as a function of adsorbent dosage (0-0.4 g/L), contact time (0-3 h), initial concentration (0.001-50 mg L^{-1}) and temperature (25-45 °C) in a batch mode. The solution pH values were adjusted to 6.0 without further adjustment during the sorption process. After adsorption process, the samples were centrifuged and filtered. The free ATP and DFC concentrations in the filtrate were detected by UV-Vis

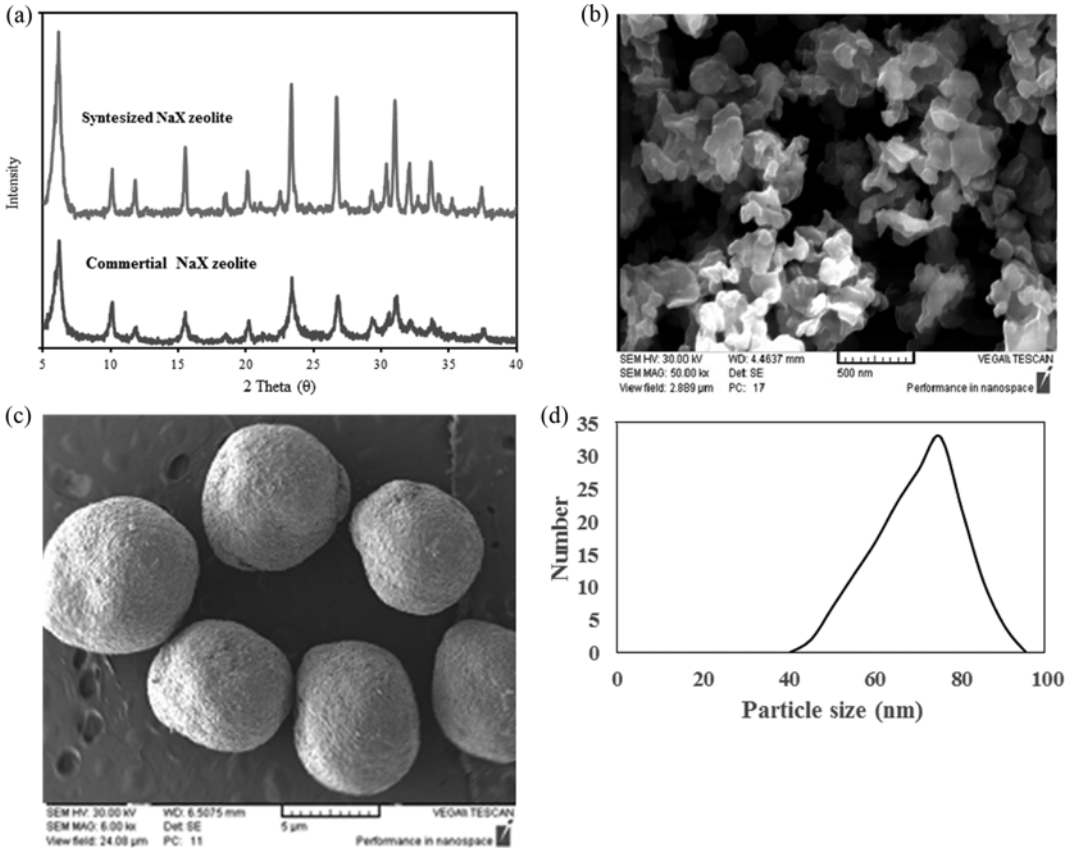

Fig. 1. (a) XRD patterns of NaX zeolite nanoparticles synthesized using microwave heating method and a commercial NaX zeolite, SEM images of (b) synthesized NaX and (c) commercial NaX zeolite particles and (d) DLS of synthesized nanoparticles.

spectrophotometer. Each experiment was repeated three times and the results were given as averages. The amount of the ATP and DCF adsorbed was calculated as follows:

$$q_e = \frac{(C_0 - C_e)V}{1000M} \quad (1)$$

where q_e is the adsorption capacity in mg g^{-1}, C_0 and C_e are the initial, and equilibrium concentrations of pharmaceutical compound in mg L^{-1}, V is the volume of the solution in mL and M is the weight of the dry adsorbent in g.

RESULTS AND DISCUSSION

1. Characterization of NaX Zeolite Nanoparticles

The X-diffraction patterns of NaX zeolite nanoparticles synthesized using microwave heating method and a commercial NaX zeolite (Zeochem) are shown in Fig. 1(a). As shown, the diffraction pattern of NaX nanoparticles and Zeochem particles match together very well. Based on Barrett-Joyner-Halenda (BJH) theory, the obtained Brunauer-Emmet-Teller (BET) surface area (S_{BET}), micropore surface area, pore volume and average pore diameter of NaX nanoparticles were found to be 560 m^2 g^{-1}, 527 m^2 g^{-1}, 0.231 cm^3 g^{-1} and 3.21 nm. By X-ray fluorescence (XRF) analysis, the Si/Al ratio of 1.30 was calculated for NaX nanozeolite. The SEM images of synthesized nanoparticles and Zeochem are shown in Fig. 1(b) and (c). The SEM images clearly proved that the zeolite crystals were morphologically similar and the sample prepared by the microwave heating was ultrafine with the average size smaller than 100 nm. Furthermore, the DLS analysis was used to evaluate the hydrodynamic diameter and particle size distribution of synthesized NaX nanozeolites (Fig. 1(d)). The particle size of 75 nm with narrow size distribution was obtained for the microwave NaX nanozeolites. The results of DLS analysis were in good agreement with the result of SEM analysis.

2. Effect of Adsorbent Dosage

The adsorbent dosage is a key parameter in the adsorption process [26]. The effect of NaX nanozeolite dosage on the adsorption of ATP and DCF for initial concentration of 10 mg L^{-1} is shown in Fig. 2. As shown, the adsorption percentages of ATP and DCF were achieved to 99.5% and 99.6% in adsorbent dosages of 0.2 and 0.25 gL^{-1}. After that, increase in adsorbent dosage did not change the adsorption efficiency remarkably. Increase in adsorbent dosage enhanced the interaction between either Na^+ cations or oxygen atoms of the zeolite with aromatic ring of ATP and DCF, which resulted in increase in the adsorption percentages of both pharmaceutical compounds. The pK_a values of DCF and ATP were 4.1 and 9.6. At pH values $\geq pK_a$, the compounds will possess negative charges. Furthermore, the pH_{pzc} of NaX nanozeolites was found to be 5.3. At pH values greater that the pH_{pzc} of NaX nanozeolites, the zeolite surface will be negatively charged. The lower adsorption of DCF compared with ATP at the same pH value (pH of 6 for both solutions of ATP and DCF) could be attributed to the electrostatic repulsion between anionic groups of DCF and negatively charged sites on the surface of NaX nanozeolites. Therefore, the adsorbent dosages of 0.2 and 0.25 gL^{-1} were selected as optimum adsorbent dosages to remove ATP and DCF from aqueous solution.

3. Effect of Contact Time and Kinetic Models

The effect of the contact time on the removal of ATP and DCF using NaX nanozeolite for initial concentration of 10 mg L^{-1} at 25 °C is presented in Fig. 3. As shown, the adsorption uptake was found to be fast at first hour for both ATP and DCF adsorption. Then, a gradual adsorption stage occurred and, subsequently, almost all of

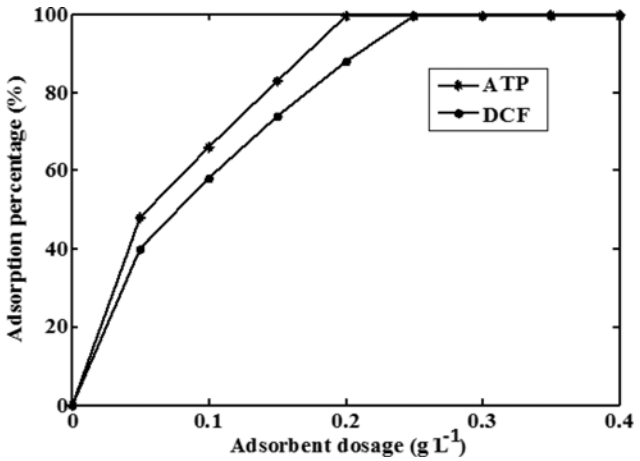

Fig. 2. Effect of NaX nanozeolite dosage on the adsorption of ATP and DCF for initial concentration of 10 mg/L.

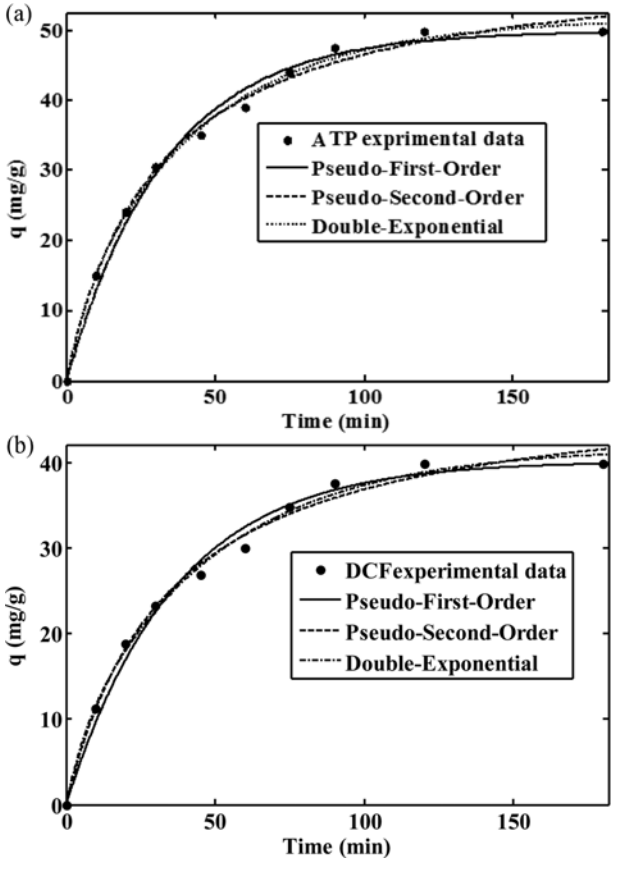

Fig. 3. Effect of contact time on the removal of (a) ATP and (b) DCF using NaX nanozeolite for initial concentration of 10 mg/L at 25 °C and kinetic models plots.

the internal and external active sites were saturated after 2 h and the system reached sorption equilibrium.

The NaX nanozeolites were free of Brönsted acid sites, excluding the model of protonated or H-bonded alcohols. However, hydrogen bonding was probably not the only interaction between zeolite and pharmaceutical compounds. The interactions between NaX nanozeolites and pharmaceutical compounds (ATP and DCF), including adsorption of ATP and DCF in the pores of zeolite NaX undergo H-bonding by hydroxyl groups to basic oxygen atoms of the NaX nanozeolites, interaction of the π electrons of the aromatic ring of the adsorbate with Na^+ cations of zeolite, interaction of the hydrogen atoms of the aromatic ring with oxygen atoms of the zeolite and interaction of ATP and DCF with silanol groups of nanozeolites by H-bonding could be responsible for adsorption of ATP and DCF onto the NaX nanozeolites. Therefore, the contact time of 2 h was selected as equilibrium time for ATP and DCF sorption.

Kinetic models, namely pseudo-first-order, pseudo-second-order and double exponential, were used to investigate the mechanism of ATP and DCF adsorption using NaX nanozeolites. These models are given by the following equations [27-29]:

$$q_t = q_e(1-\exp(-k_1 t)) \quad (2)$$

$$q_t = \frac{k_2 q_e^2 t}{1+k_2 q_e t} \quad (3)$$

$$q_t = q_e - \frac{D_1}{x_{ads}}\exp(-k_{D1}t) - \frac{D_2}{x_{ads}}\exp(-k_{D2}t) \quad (4)$$

where q_t and q_e (mg g^{-1}) are the adsorption capacity at time t and equilibrium time. k_1 (min^{-1}) and k_2 (g mg^{-1} min^{-1}) are the pseudo-first-order and pseudo-second-order models constants. D_1 and D_2 (mg L^{-1}) are the constants of the rapid and slow steps and k_{D1} and k_{D2} (min^{-1}) are constant controlling the mechanism and x_{ads} (g L^{-1}) is the adsorbent concentration. The parameters of kinetic models are presented in Table 1.

By contrasting correlation coefficients for kinetic models, the kinetic data was best described by double exponential kinetic model (R^2>0.995). By examining the values of constant parameters of double-exponential kinetic model, both external diffusion and internal diffusion are effective in the ATP and DCF sorption by NaX nanozeolites.

4. Effect of Initial Concentration and Isotherm Models

The effects of the initial concentrations of ATP and DCF (0.001-50 mg L^{-1}) on the adsorption capacity of NaX zeolite at three different temperatures (25, 35, 45 °C) are shown in Fig. 4. As shown, the adsorption capacity of ATP and DCF was increased by raising temperatures. It indicated that the removal of ATP and DCF onto the NaX nanozeolites was favorable at higher temperatures. Isotherm models, including Freundlich, Langmuir, Temkin and Dubinin-Radushkevich (D-R), were used to describe the equilibrium data of ATP and DCF using NaX nanozeolite. These models are given by Eqs. (5), (6), (7) and (8), respectively [30-33]:

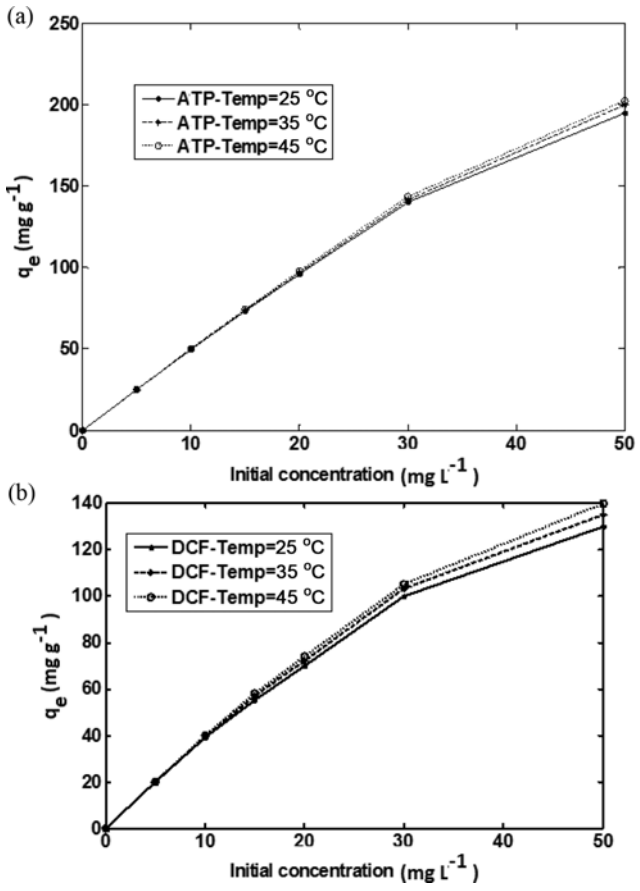

Fig. 4. Effect of the initial concentration of (a) ATP and (b) DCF at three different temperatures.

$$q_e = k_F C_e^{1/n} \quad (5)$$

$$q_e = q_m \frac{bC_e}{1+bC_e} \quad (6)$$

$$q_e = B \ln(A_T C_e) \quad (7)$$

$$q_e = q_{DR}\exp(-B_{DR}\varepsilon_{DR}^2) \quad (8)$$

where k_F (mg g^{-1}) and n are the Freundlich parameters. q_m (mg g^{-1}) is the maximum adsorption capacity of adsorbent that is related to the monolayer adsorption capacity and b (L mg^{-1}) is the Langmuir

Table 1. Kinetic parameters of ATP and DCF using NaX nanozeolite

Sample	Pseudo-first-order			Pseudo-second-order			Double-exponential					
	q_{eq} (mg g^{-1})	k_1 (min^{-1})	R^2	q_{eq} (mg g^{-1})	k_2 (g mg^{-1}·min^{-1})	R^2	q_{eq} (mg g^{-1})	D_1 (mgL^{-1})	k_{D1} (min^{-1})	D_2 (mgL^{-1})	k_{D2} (min^{-1})	R^2
ATP	49.81	0.0301	0.990	60.63	0.000544	0.993	51.63	1.658	0.150	8.674	0.023	0.996
DCF	40.14	0.0275	0.988	49.39	0.000595	0.991	41.76	1.259	0.153	7.101	0.020	0.995

Table 2. Isotherm parameters of ATP and DCF at different temperatures

Sample	T (°C)	Freundlich isotherm			Langmuir isotherm			Temkin isotherm			D-R isotherm		
		K_F (mg g^{-1})	n	R^2	q_{max} (mg g^{-1})	K_L (L mg^{-1})	R^2	B_T	A_T	R^2	q_{DR} (mmol g^{-1})	B_{DR} (mol^2 J^{-2})	R^2
ATP	25	119.21	1.931	0.93	328.4	0.433	0.87	32.9	66.2	0.77	1.732	6.021×10^{-9}	0.78
	35	138.40	2.145	0.93	336.2	0.698	0.86	26.5	247.3	0.73	1.775	5.321×10^{-9}	0.80
	45	165.42	2.201	0.94	350.3	1.273	0.83	25.0	505.6	0.68	1.858	2.422×10^{-9}	0.77
DCF	25	64.57	2.439	0.97	216.6	0.309	0.90	20.4	63.2	0.80	1.047	7.651×10^{-9}	0.86
	35	73.17	2.464	0.97	218.5	0.402	0.88	20.9	82.9	0.80	1.155	6.727×10^{-9}	0.85
	45	82.43	2.645	0.97	221.0	0.649	0.88	21.1	110.2	0.85	1.267	5.498×10^{-9}	0.81

model constant. B (RT/b_T) is Temkin constant related to heat of adsorption and A_T (L/g) is equilibrium binding constant related to maximum binding energy. q_{DR} (mg g^{-1}) and B_{DR} (mol^2 J^{-2}) are the D-R isotherm constants and ε_{DR} is the Polanyi potential that is equal to RT ln(1+1/C_e). R is the gas constant (8.314 J mol^{-1} K^{-1}) and T is the absolute temperature (K). The value of B_{DR} is related to the adsorption free energy that can be calculated from the following equation:

$$E = \frac{1}{\sqrt{2B_{DR}}} \quad (9)$$

The value of free energy determines the type of adsorption mechanism. If E value lies between 8 and 16 kJ mol^{-1} the adsorption process proceeds chemisorption mechanism, and while E value is 8 kJ mol^{-1}, the adsorption process mechanism is physical [25]. The values of isotherm parameters are obtained by nonlinear regression using MATLAB software and results are given in Table 2.

The comparison of R^2 values of Freundlich (R^2>0.93), Langmuir (R^2>0.83), Temkin (R^2>0.68) and Dubinin-Radushkevich (R^2>0.77) at different studied temperatures indicated that the Freundlich isotherm models described best the equilibrium data of DCF and ATP data. The results of E values of D-R isotherm revealed that the sorption mechanism of both of ATP (9.11<E<14.37) and DCF (8.08< E<9.53) using NaX nanozeolite was chemisorption.

The maximum adsorption capacities of ATP and DCF onto the NaX nanozeolites are compared with other adsorbents reported in the literature [34-39] and is listed in Table 3. As shown, the adsorption capacity of NaX nanozeolites for ATP and DCF was found to be comparable and moderately higher than those of many corresponding sorbents in the literature.

5. Thermodynamic Parameters

Thermodynamic parameters including (Gibbs free energy change (ΔG^o), enthalpy change (ΔH^o) and entropy change (ΔS^o) are calculated by the following equations:

Table 3. Comparison of adsorption capacity (mg g^{-1}) of NaX nanozeolites adsorbent with other adsorbents for the ATP and DCF sorption

Adsorbent	Adsorbate	Adsorption capacity (mg g^{-1})	Ref.
S/0.5:1/700	ATP	120.5	33
S/0.5:1/800	ATP	124.5	33
VP	ATP	119.1	33
NSAES	ATP	151.9	33
Pi/1:1/800/2	ATP	270.3	34
Pi/1:3/800/2	ATP	434.8	34
Pi-fa/1:1/800	ATP	188.7	35
Pi-fa/1:3/800	ATP	243.9	35
Pi-fa/1:1/900	ATP	200.0	35
Pi-fa/1:3/900	ATP	270.3	35
NaX nanozeolites	ATP	350.3	In this study
Grape bagasse	DCF	76.98	36
MIP	DCF	324.8	37
HMS	DCF	31.93	38
M-HMS	DCF	35.59	38
SBA-15	DCF	34.18	38
MCM-41	DCF	32.64	38
PAC	DCF	40.55	38
NaX nanozeolites	DCF	221.0	In this study

$$k_C = \lim_{C_{el}\to 0} \frac{C_{es}}{C_{el}} \quad (10)$$

$$\Delta G^o = -RT \ln k_C \quad (11)$$

$$\ln k_C = \frac{\Delta S^o}{R} - \frac{\Delta H^o}{RT} \quad (12)$$

where R is the gas constant (8.314 J $mol^{-1}\cdot K^{-1}$), T is an absolute

Table 4. Thermodynamic parameters of ATP and DCF sorption using NaX zeolite

Sample	k_C			ΔH^o (kJ mol^{-1})	ΔS^o (kJ mol^{-1} K^{-1})	ΔG^o (kJ mol^{-1})		
	25 °C	35 °C	45 °C			25 °C	35 °C	45 °C
ATP	278.0	1408.3	1780.3	73.71	0.296	−13.493	−18.561	−19.789
DCF	232.3	343.3	525.3	32.14	0.153	−13.490	−14.951	−16.561

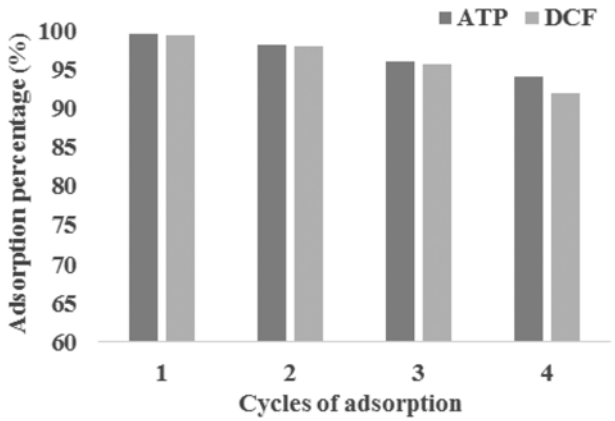

Fig. 5. Reusable ability of NaX nanozeolites with 0.1 M HNO_3.

temperature (K) and k_C is the adsorption equilibrium constant. C_{es} and C_{el} are the values of solid phase concentration and liquid phase concentration at equilibrium in mgL^{-1}. The results are presented in Table 4. As shown, all the Gibbs free energy change values were negative. This indicated the feasibility and spontaneous natures of ATP and DCF sorption using NaX nanozeolites. Furthermore, the degree of spontaneity of the reaction increased by raising temperature, indicating the greater feasibility of adsorption process at higher temperatures.

The positive values of ΔH^o and ΔS^o revealed the endothermic nature of ATP and DCF sorption using NaX nanozeolite and increasing the randomness of solid-solution interface during the adsorption process, respectively.

6. Desorption and Reusability

Four cycles of adsorption-desorption of ATP and DCF molecules by NaX nanozeolites in the initial concentration of 10 mg L^{-1} and 25 °C were investigated, which results are shown in Fig. 5. The desorption step of ATP and DCF from NaX nanozeolites was treated with 0.1 M HNO_3 solution. Desorption time was fixed as 2 h throughout the adsorption period. As shown, the removal percentages for ATP and DCF were observed to decrease by increasing the cycles of adsorption. Whereas, the differences between sorption percentages for both ATP and DCF molecules in first and four cycles were lower than 10%. The adsorption/desorption tests revealed that NaX nanozeolites is an efficient adsorbent for ATP and DCF removal.

CONCLUSION

The performance of NaX nanozeolite synthesized by microwave heating method for adsorption of ATP and DCF was investigated. The synthesis of NaX zeolite indicated that the Si/Al ratio of nanozeolites was 1.3. The SEM image of zeolite demonstrated that the prepared zeolite had narrow size distribution with the average particle size diameter of 61 nm. The surface area of NaX zeolite nanoparticles based on BET analysis was 560 $m^2 g^{-1}$. The effect of time on adsorption of ATP and DCF using NaX zeolite indicated that the obtained equilibrium time was 2 h. The kinetic and equilibrium data of ATP and DCF adsorption using NaX zeolite were well described using double exponential kinetic and Freundlich isotherm models, respectively. The results indicated that the adsorption efficiencies of ATP and DCF followed a descending order: ATP>DCF. The calculated thermodynamic parameters showed the feasibility, endothermic and spontaneous nature of ATP and DCF using NaX zeolite at studied conditions. The adsorption percentages of ATP and DCF did not change remarkably after four sorption-desorption cycles.

REFERENCES

1. K. Kümmerer, *J. Environ. Manage.*, **90**, 2354 (2009).
2. I. Sirés and E. Brillas, *Environ. Inter*, **40**, 212 (2012).
3. S. Esplugas, D. M. Bila, L. G. T. Krause and M. Dezotti, *J. Hazard. Mater.*, **149**, 631 (2007).
4. P. Bartels and W. Von Tümpling, *Sci. Total Environ.*, **374**, 143 (2007).
5. Y. Kim, K. Choi, J. Jung, S. Park, P.-G. Kim and J. Park, Envi*ron. Int.*, **33**, 370 (2007).
6. L. Yang, L. E. Yu and M. B. Ray, *Water Res.*, **42**, 3480 (2008).
7. A. Agüera, L. A. Pérez-Estrada, I. Ferrer, E. M. Thurman, S. Malato and A. R. Fernández-Alba, *J. Mass Spectrom.*, **40**, 908 (2005).
8. A. Y. C. Lin and Y. T. Tsai, *Sci. Total Environ.*, **407**, 3793 (2009).
9. S. Bae, D. Kim and W. Lee, *Appl. Catal. B: Environ.*, **134**, 93 (2013).
10. K. Rzeszutek and A. Chow, *Talanta*, **46**, 507 (1998).
11. A. P. Annachhatre and S. H. Gheewala, *Biotechnol. Adv.*, **14**, 35 (1996).
12. C. Mc. Manamon, J. D. Holmes and M. A. Morris, *J. Hazard. Mater.*, **193**, 120 (2011).
13. T. X. Bui, S.-Y. Kang, S.-H. Lee and H. Choi, *J. Hazard. Mater.*, **193**, 156 (2011).
14. N. Klamerth, K. Rizzo, S. Malato, M. I. Maldonado, A. Aguera and A. R. Fernandez-Alba, *Water Res.*, **44**, 545 (2010).
15. L. C. Almeida, S. Garcia-Segura, N. Bocchi and E. Brillas, *Appl. Catal. B: Environ.*, **103**, 21 (2011).
16. M. D. G. de Luna, M. L. Veciana, C. C. Su and M. C. Lu, *J. Hazard. Mater.*, **217**, 200 (2012).
17. T. X. Bui and H. Choi, *J. Hazard. Mater.*, **168**, 602 (2009).
18. Z. Yu, S. Peldszus and P. M. Huck, *Water Res.*, **42**, 2873 (2008).
19. A. Rossner, S. A. Snyder and D. R. U. Knappe, *Water Res.*, **43**, 3787 (2009).
20. T. X. Bui and H. Choi, *J. Hazard. Mater.*, **168**, 602 (2009).
21. M. Antunes, V. I. Esteves, R. Guégan, J. S. Crespo, A. N. Fernandes and M. Giovanela, *Chem. Eng. J.*, **192**, 114 (2012).
21. S. M. Rivera-Jimenez, S. Mendez-Gonzalez and A. Hernandez-Maldonado, *Micropor. Mesopor. Mater.*, **132**, 470 (2010).
22. M. Khalid, G. Joly, A. Renaud and P. Magnoux, *Ind. Eng. Chem. Res.*, **43**, 3275 (2004).
23. B. Z. Zhan, M. A. White, K. N. Robertson, T. S. Camerona and M. Gharghourib, *Chem. Commun.*, **13**, 1176 (2001).
24. M. Ansari, A. Aroujalian, A. Raisi and M. Fathizadeh, *Adv. Powder. Technol.*, **25**, 722 (2014).
25. M. Irani, A. R. Keshtkar and M. A. Mousaviana, *Chem. Eng. J.*, **175**, 251 (2011).
26. M. Irani, A. R. Keshtkar and M. A. Mousavian, *Korean J. Chem. Eng.*, **29**, 1459 (2012).
27. S. Lagergren, *Handlingar*, **24**, 1 (1898).
28. Y. S. Ho and G. McKay, *Process. Biochem.*, **34**, 451 (1999).
29. N. Chiron, R. Guilet and E. Deydier, *Water Res.*, **37**, 3079 (2003).

30. H. M. F. Freundlich, *J. Phys. Chem*., **57**, 385 (1906).
31. I. Langmuir, *J. Am. Chem. Soc*., **38**, 2221 (1916).
32. M. I. Temkin and V. Pyzhev, *Acta Physiochim*., **URSS 12**, 327 (1940).
33. M. M. Dubinin, E. D. Zaverina and L. V. Radushkevich, *Zhurnal Fizicheskoi Khimii*, **21**, 1351 (1947).
34. A. S. Mestre, A. S. Bexiga, M. Proença, M. Andrade, M. L. Pinto, I. Matos, I. M. Fonseca and A. P. Carvalho, *Bioresour. Technol.*, **102**, 8253 (2011).
35. M. Galhetas, A. S. Mestre, M. L. Pinto, I. Gulyurtlu, H. Lopes and A. P. Carvalho, *J. Colloid Interface Sci*., **433**, 94 (2014).
36. M. Galhetas, A. S. Mestre, M. L. Pinto, I. Gulyurtlu, H. Lopes and A. P. Carvalho, *Chem. Eng. J*., **240**, 344 (2014).
37. M. Antunes, V. I. Esteves, R. Guégan, J. S. Crespo, A. N. Fernandes and M. Giovanela, *Chem. Eng. J*., **192**, 114 (2012).
38. C. M. Dai, S. U. Geissen, Y. L. Zhang, Y. J. Zhang and X. F. Zhou, *Environ. Pollut.*, **159**, 1660 (2011).
39. N. Suriyanon, P. Punyapalakul and C. Ngamcharussrivichai, *Chem. Eng. J*., **214**, 208 (2013).